# REPORT DOCUMENTATION PAGE

*Form Approved*
*OMB No. 0704-0188*



**1. REPORT DATE** *(DD-MM-YYYY)*
05-21-04

**2. REPORT TYPE**
Technical Paper

**3. DATES COVERED** *(From - To)*

**4. TITLE AND SUBTITLE**

**A Photoelastic Study of Cracking in Motor Grain Models**

**5a. CONTRACT NUMBER**

**5b. GRANT NUMBER**

**5c. PROGRAM ELEMENT NUMBER**

**6. AUTHOR(S)**

C.W. Smith, J.D. Hansen

**5d. PROJECT NUMBER**
2302

**5e. TASK NUMBER**
0378

**5f. WORK UNIT NUMBER**
23020378

**7. PERFORMING ORGANIZATION NAME(S) AND ADDRESS(ES)**

Air Force Research Laboratory (AFMC)
AFRL/PRS
5 Pollux Drive
Edwards AFB, CA 93524-7048

**8. PERFORMING ORGANIZATION REPORT NUMBER**

**9. SPONSORING / MONITORING AGENCY NAME(S) AND ADDRESS(ES)**

Air Force Research Laboratory (AFMC)
AFRL/PRS
5 Pollux Drive
Edwards AFB, CA 93524-7048

**10. SPONSOR/MONITOR'S ACRONYM(S)**

**11. SPONSOR/MONITOR'S NUMBER(S)**
AFRL-PR-ED-VG-2004-178

**12. DISTRIBUTION / AVAILABILITY STATEMENT**

Approved for public release; distribution unlimited.

**13. SUPPLEMENTARY NOTES**
SEM X International Congress & Exposition on Experimental And Applied Mechanics
Costa Mesa, CA. 7-10 Jun 2004

**14. ABSTRACT**

20040715 193

**15. SUBJECT TERMS**

| 16. SECURITY CLASSIFICATION OF: | | | 17. LIMITATION OF ABSTRACT | 18. NUMBER OF PAGES | 19a. NAME OF RESPONSIBLE PERSON |
|---|---|---|---|---|---|
| | | | | | Linda Talon |
| a. REPORT | b. ABSTRACT | c. THIS PAGE | | | 19b. TELEPHONE NUMBER *(include area code)* |
| Unclassified | Unclassified | Unclassified | A | 10 | (661) 275-5283 |



**BEST AVAILABLE COPY**

# A PHOTOELASTIC STUDY OF CRACKING IN MOTOR GRAIN MODELS

C. W. Smith and J. D. Hansen

Department of Engineering Science and Mechanics
Virginia Polytechnic Institute and State University
Blacksburg, Virginia 24061-0219

length of cylinder 376 mm

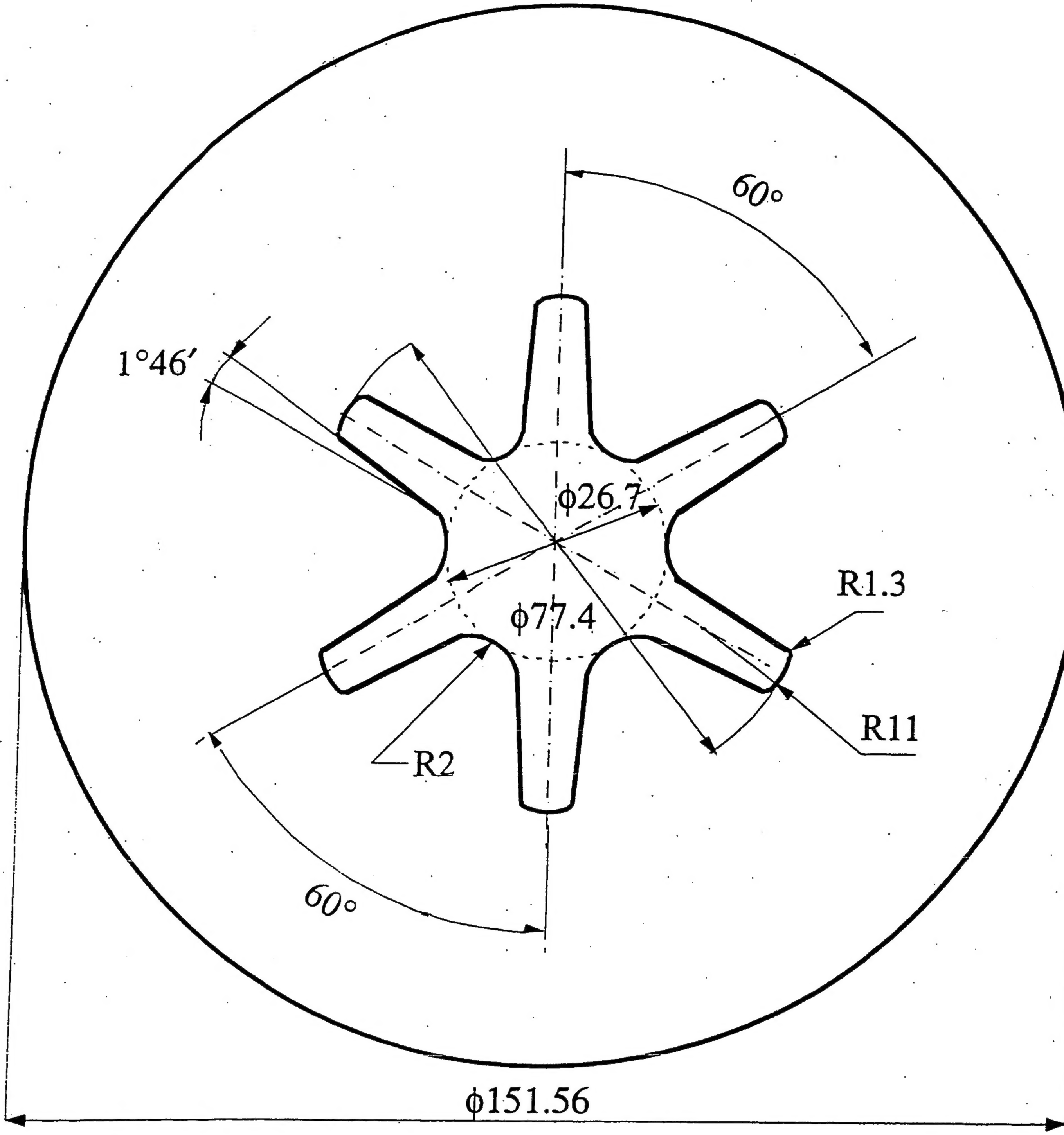


all dimensions are in mm

Figure 2: Crosssection of test models.

3

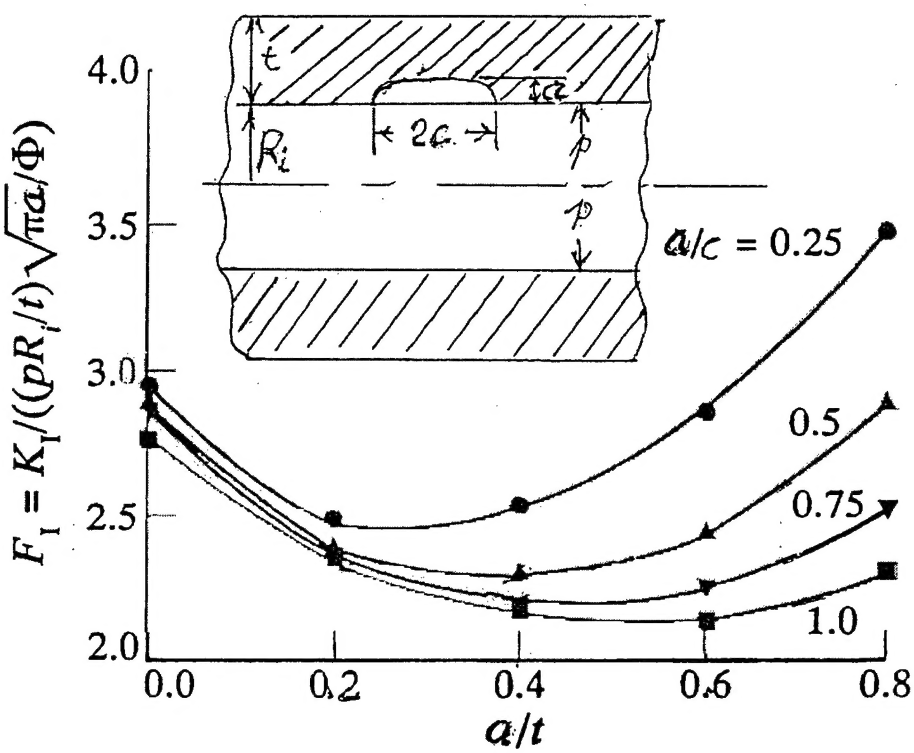


(b) $t/R_i = 1.0$

- Results from BEM showing "dish" shaped region for normalized SIF for a semi-elliptic surface crack in a pressurized thick walled cylinder.

- $F_I$ - $K_I$ = SIF; p = pressure, $\Phi$ = Elliptic Integral of Second Kind. See Table 1 slide.

# Model 3

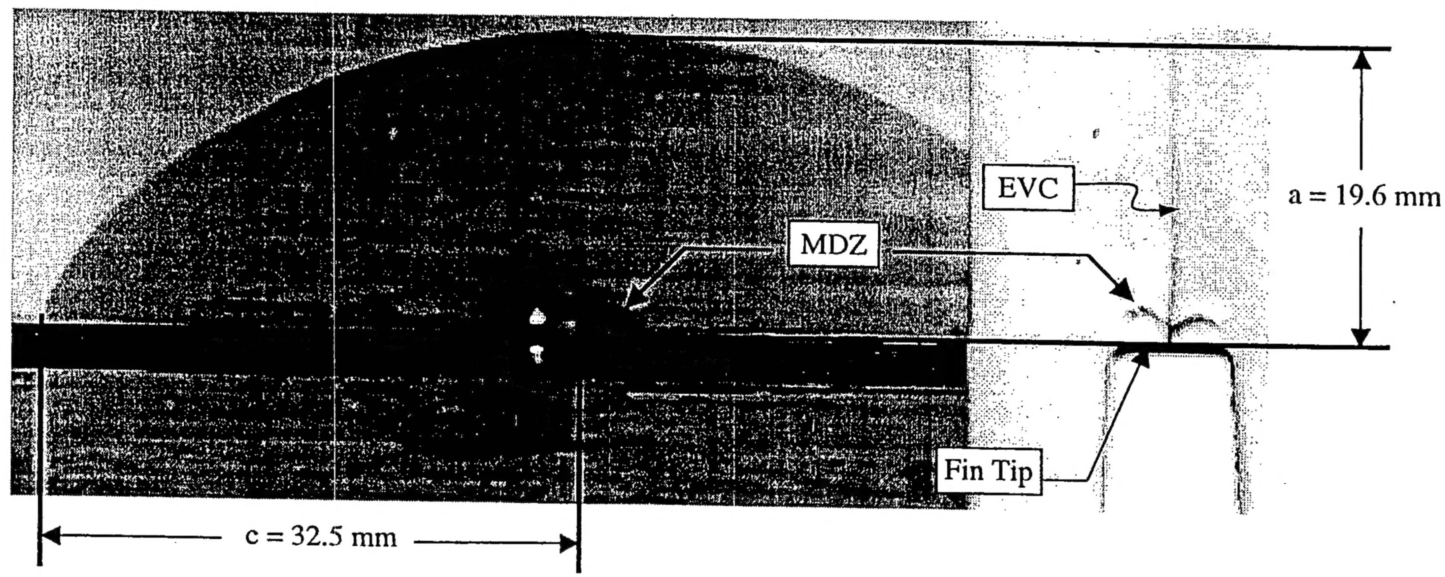


MDZ – Material Damage Zone
EVC – Edge View of Crack

Figure 3: Crack shape and fin tip location for model 3

# Model 6b

**Center Slice (t = 4.29 mm)**

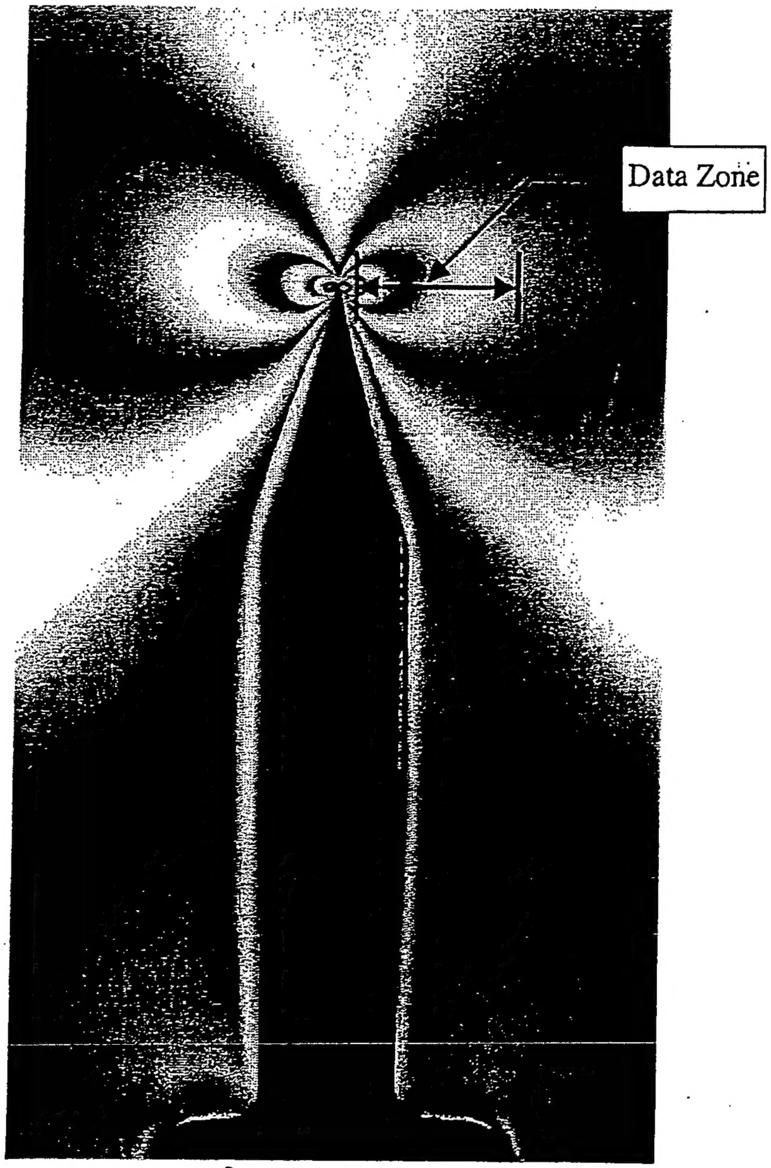


| | |
|---|---|
| $P_{sf}$: | $2.3 \times 10^{-2}$ MPa |
| $c_f$: | 175.30 mm |
| $a_f$: | 19.6 mm |
| Data zone: | $(r_{ave})_2 - (r_{ave})_1 = 4.2635 - 0.4564 = 3.807$ mm |

Figure 4: Unmultiplied fringe pattern from a 4.3mm slice from the center of the crack for Model 6 using a diffused light polariscope for a machined crack denoting location of data zone.

## Mode I Algorithm For Determination of Stress Intensity Factor (SIF)

In linear elastic fracture mechanics (LEFM) using the photoelastic approach, one can begin with Mode I near tip equations (Fig. A-1)

$$\sigma_{ij} = \frac{K_I}{\sqrt{8\pi r}} f_{ij}(\theta) + \sigma^{\circ}_{ij} \quad (i.j. = n, z) \tag{A-1}$$

where $K_I$ is the Mode I SIF, $\sigma^{\circ}_{ij}$ are the contribution of the nonsingular stresses in the measurement zone, and $r, \theta$ then are centered at the crack tip. The following expression is computed, in truncated form, along $\theta = \pi/2$, where fringe spreading is greatest. (Fig. A-2) Thus

$$\tau^{nz}_{max} = \frac{K_{AP}}{\sqrt{8\pi r}} = \frac{K_I}{\sqrt{8\pi r}} + \tau_0 \tag{A-2}$$

where $K_{AP}$ is an "apparent" SIF, which includes the effect of $\sigma^{\circ}_{ij}$ {i.e., $\tau_0 = f(\sigma^{\circ}_{ij})$} with the singular effect in the measurement zone. The stress-optic law states that $\tau^{nz}_{max} = \frac{N_f}{2t}$, where $N$ is the measured stress fringe order, $f$ is the material fringe value and $t$ the slice thickness. Thus $\tau^{nz}_{max}$ is proportional to $N$ and may be regarded as the measured quantity together with $r$. By rearranging terms in Eq. A-2 and normalizing, we can obtain

$$\frac{K_{AP}\Phi}{p\sqrt{\pi a}} = \frac{K_I \Phi}{p\sqrt{\pi a}} + \frac{\sqrt{8}}{p}\tau_o \Phi \left(\sqrt{\frac{r}{a}}\right) \tag{A-3}$$

for a semi-elliptic crack where the coefficient of $\sqrt{r/a}$ is a constant, $p$ is the internal pressure and $a$ is the crack size. $\Phi$ is an elliptic integral which varies with the aspect ratio of the crack (a/c). Its form is approximated by $\sqrt{Q}$ where $Q$ is given in Table I. In general, when applied to cylindrical vessels, the denominator of Eq. A-3 should be $p\frac{R_i}{t}$. However, in the present problem geometry, $R_i/t = 1$, and the $R_i/t$ can be dropped here.

By defining the normalized SIF as

$$F = \frac{K_{AP}\sqrt{Q}}{p\sqrt{\pi a}} \tag{A-4}$$

one can plot $F$ vs. $\sqrt{r/a}$ and locate the linear zone implied by Eq. A-3, which is the zone dominated by the stress singularity. By extending this line to the origin, the value of $F$ is determined as shown in Fig. A.3 for Model 1.

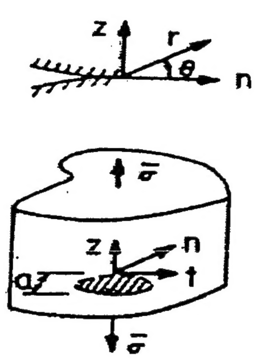


Fig. A-1: Mode I Near Tip Notation

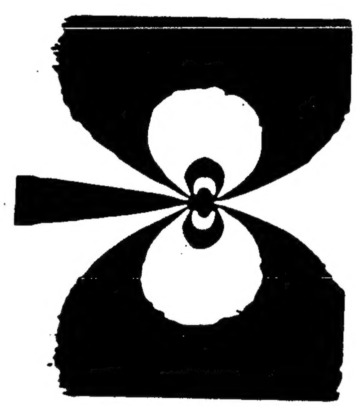

Fig. A-2: Mode I Fringe (Pattern Unmultiplied)

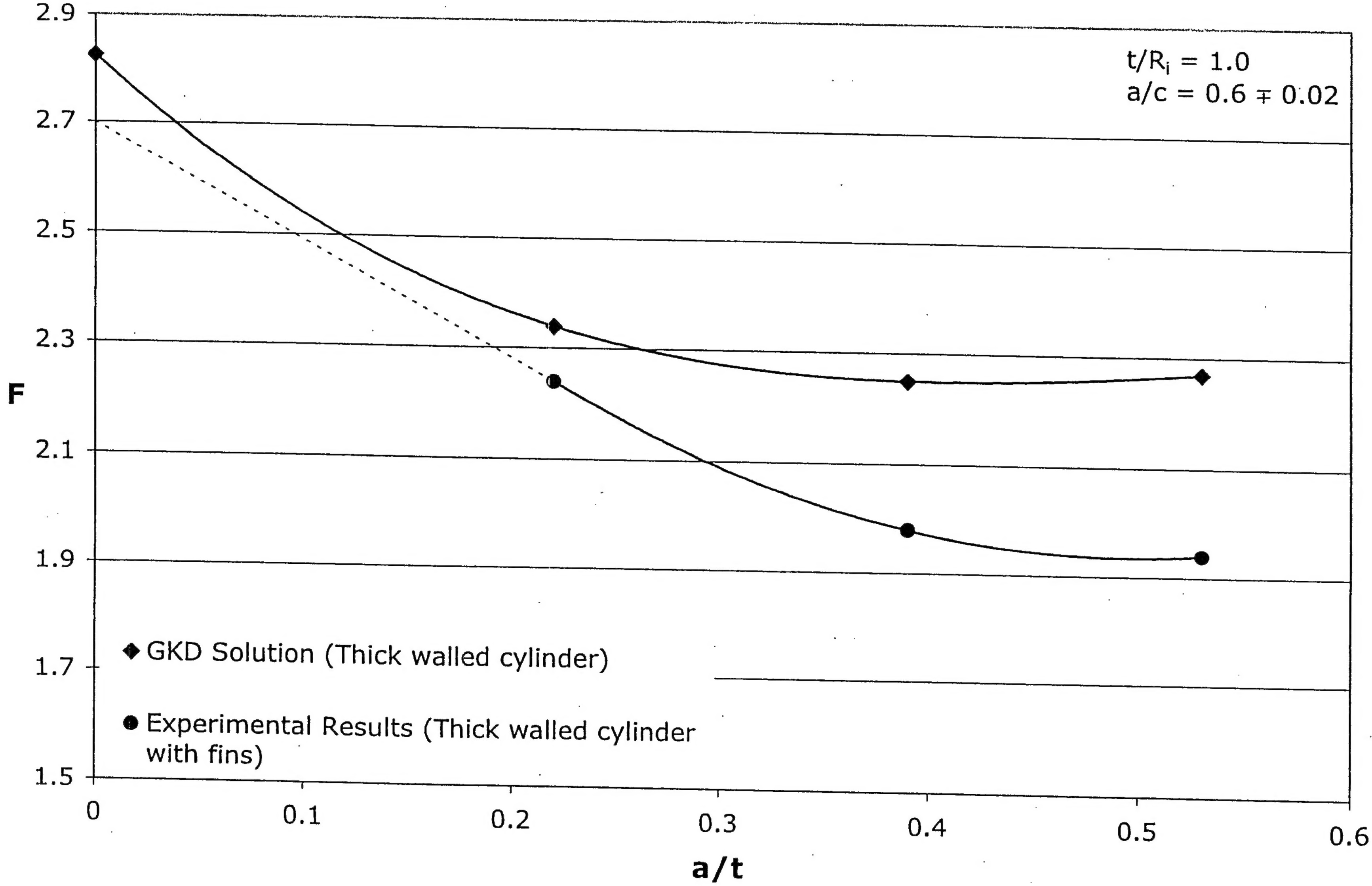


Figure 5: Comparison of experimental results for part through cracks in star finned models with same depth cracks in the pressurized cylinder models (GKD) in the central "dish bottom" region.

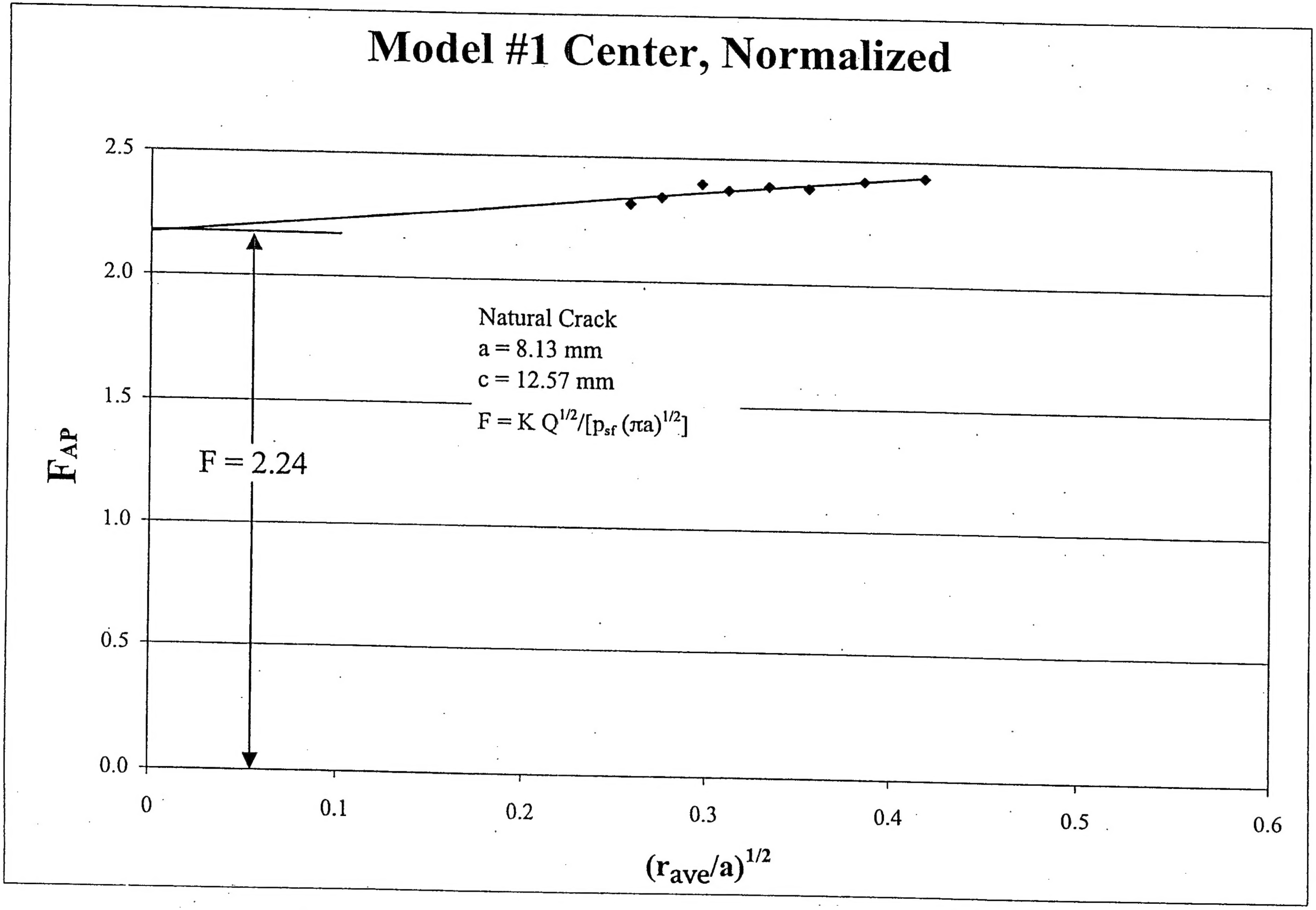


Figure A-3: Determination of Normalized Stress Intensity Factor (F) from Test Data.

## Table 1

### Test Data and Computed Results

| Col | 1 | 2 | 3 | 4 | 5 | 6 | 7 | 8 | 9 | 10 | 11 | 12 | 13 | 14 |
|---|---|---|---|---|---|---|---|---|---|---|---|---|---|---|
| Test | a | c | a/c | a/t | $\rho_{sf}$ | $\rho_{max}$ | $K_{EXP}$ | $K_{GKD}$ | $K_{BF}$ | $K_{PSE}$ | $F_{GKD}$ | $F_{BF}$ | $F_{EXP}$ | $F_{PSE}$ |
| 1 | 8.13 | 12.57 | 0.65 | 0.22 | 0.041 | 0.121 | 0.35 | 0.37 | 0.57 | 0.55 | 2.34 | 2.77 | 2.24 | 2.65 |
| 2 | 14.6 | 23.00 | 0.63 | 0.39 | 0.046 | 0.129 | 0.47 | 0.54 | 0.93 | 0.82 | 2.25 | 2.99 | 1.98 | 2.63 |
| 3* | 19.6 | 32.50 | 0.60 | 0.53 | 0.028 | 0.167 | 0.33 | 0.39 | 0.70 | 0.60 | 2.27 | 3.17 | 1.94 | 2.71 |
| 4 | 8.31 | 183.24 | 0.05 | 0.22 | 0.041 | 0.041 | 0.46 | 0.56 | 0.58 | 0.48 | 2.70 | 2.77 | $2.22^{+}$ | 2.28 |
| 5 | 14.6 | 181.65 | 0.08 | 0.39 | 0.041 | 0.041 | 0.68 | 0.73 | 0.83 | 0.78 | 2.65 | 2.99 | $2.49^{+}$ | 2.81 |
| 6 | 19.6 | 175.30 | 0.11 | 0.53 | 0.023 | 0.023 | 0.44 | 0.48 | 0.57 | 0.52 | 2.70 | 3.17 | $2.47^{+}$ | 2.90 |

Linear dimensions -mm

Pressure $= N/mm^2$

$$F = \frac{K_1\sqrt{Q}}{pR_i/t)\sqrt{\pi a}} : \sqrt{Q} = \phi = \text{elliptic Integral of 2nd kind}$$

$K$ values $= \frac{N}{mm^{3/2}}$

$R_i$ = Inner cylinder radius $Q \approx 1 + 1.464\left(\frac{a}{c}\right)^{1.65} \quad \frac{a}{c} < 1$

$\rho_{sf}$ = Stress freezing pressure $\quad t$ = Cylinder wall thickness or (distance from fin tip to outer boundary)

subscript notations

KGD = Gouzhong, Kangda and Dongdi (For Cyl.)

BF = Bowie & Freese (for Cyl.)

$$K_{PSE} = K_{EXP}\left(\frac{K_{BF}}{K_{GKD}}\right)$$

+ These crack shapes were not semi-elliptical or through the length cracks.

* Cylinder length was 336mm

# Summary

By capitalizing on observed similarities between the cracked finned model and a cracked cylinder when placing the fin tip at the inner edge of the cylinder, estimates were made by assuming a plane strain solution for the finned model in finite length models. Based upon the aforementioned limited results, use of a modified plane strain solution appears to yield a slightly conservative prediction for long shallow cracks to significantly conservative prediction for deep part-through cracks.